

Microencapsulation of cellular aggregates composed of differentiated insulin and glucagon-producing cells from human mesenchymal stem cells derived from adipose tissue.

Claudia Jara

Universidad de Chile

Felipe Oyarzun-Ampuero

Universidad de Chile

Flavio Carrión

Universidad del Desarrollo

Esteban González-Echeverría

Universidad de Chile

Claudio Cappelli

Universidad Austral de Chile

Pablo Caviedes (✉ pablo.caviedes@cicef.cl)

Universidad de Chile Facultad de Medicina <https://orcid.org/0000-0003-4462-7422>

Research

Keywords: Adipose-derived mesenchymal stem cells, Cellular aggregates, Cellular Differentiation, Cell Therapy, Diabetes, Microencapsulation

Posted Date: July 27th, 2020

DOI: <https://doi.org/10.21203/rs.3.rs-22053/v3>

License:   This work is licensed under a Creative Commons Attribution 4.0 International License.

[Read Full License](#)

Version of Record: A version of this preprint was published on August 5th, 2020. See the published version at <https://doi.org/10.1186/s13098-020-00573-9>.

Abstract

Background: In type I diabetes mellitus (T1DM) pancreatic β cells are destroyed. Treatment entails exogenous insulin administration and strict diet control, yet optimal glycemic control is hardly attainable. Islet transplant could be an alternative in patients with poor glycemic control, but inefficient islet purification and autoimmune response of patients is still a challenge. For these reasons, it is necessary to explore new cellular sources and immunological isolation methods oriented to develop T1DM cell-based therapies.

Aims: We postulate human adipose-derived stem cell (hASC) as an adequate source to generate pancreatic islet cells *in vitro*, and to produce islet-like structures. Furthermore, we propose microencapsulation of these aggregates as an immunological isolation strategy.

Methods: hASC obtained from lipoaspirated fat tissue from human donors were differentiated *in vitro* to insulin (Ins) and glucagon (Gcg) producing cells. Then, insulin producing cells (IPC) and glucagon producing cells (GPC) were later cocultured in low adhesion conditions to form cellular aggregates, and later encapsulated in a sodium alginate polymer. Expression of pancreatic lineage markers and secretion of insulin or glucagon *in vitro* were analyzed.

Results: The results show that multipotent hASC efficiently differentiate to IPC and GPC, and express pancreatic markers, including insulin or glucagon hormones which they secrete upon stimulation (5 fold for insulin in IPC, and 4 fold for glucagon, compared to undifferentiated cells. In turn, calculation of the Feret diameter and area of cellular aggregates revealed, finding mean diameters $\sim 80 \mu\text{m}$ and 65 % of the aggregates reached $4000 \mu\text{m}^2$ at 72h of formation. IPC/GPC aggregates were then microencapsulated in sodium-alginate polymer microgels, which were found to be more stable when stabilized with Ba^{2+} , yielding average diameters $\sim 300 \mu\text{m}$. Interestingly, Ba^{2+} -microencapsulated aggregates respond to high external glucose with insulin secretion.

Conclusions: The IPC/GPC differentiation process from hASC, followed by the generation of cellular aggregates that are later microencapsulated, could represent a possible treatment for T1DM.

1. Background

Type I diabetes mellitus (T1DM) is an autoimmune and degenerative disease characterized by an autoimmune reaction against pancreatic β cells [1]. Glycemic control by conventional parenteral insulin (Ins) therapy accompanied by strict diet and controlled physical exercise is often inefficient, as the loss of β cells entails the absence of paracrine regulation between α and β cells exists [2].

A promising therapy had been proposed by results from the Edmonton protocol, which utilized glucocorticoid-free immunosuppression combined with infusion of an adequate mass of freshly prepared post-mortem pancreatic islets. With this treatment, 44% of treated subjects became insulin independent after one year of transplantation [3]. However, at present, this therapy is restricted to patients with poor or no metabolic control [4, 5]. Indeed, the shortage of donors and technical limitations entailed in pancreatic

islet isolation make the massive implementation of this therapy difficult [6]. Also, activation of the immune system against the transplanted islets results in the gradual death of the graft [6]. Further, immunosuppressants used, such as tacrolimus and/or sirolimus, are diabetogenic, and reportedly have other undesirable side effects such as mouth ulcers, diarrhea and acne [7]. Recently, new immunosuppression protocols have been tested, which include different T and B-cell depleting agents, and immunosuppressors [8]. In addition to the use of long-term glucocorticoid-free immunosuppressants, immunological isolation of the graft by encapsulation has been proposed as a solution [6]. On the other hand, encapsulation in pancreatic islet provides a physical barrier against immune system activation [9]. Thus, it is essential to find new cellular sources and immunological isolation methods to face these limitations.

As a cellular source, we propose the use of mesenchymal stem cells (MSC), a population of multipotent cells present in almost all adult tissues [10]. MSC cells derived from adipose tissue, or "adipose-derived stem cells" (hASC) are easier to purify by using less invasive methods [11, 12]. Previous studies showed that hASC can be differentiated to insulin producing cells (IPC), [13, 14] and glucagon producing cells (GPC) [15] independently. Other groups have reported generation of islets-like cell aggregates (ICA) [16, 17] to reestablish not only β -cell function, but also part of the necessary paracrine regulation between α and β cells [18]. However, the activation of the immune system against grafts remains a major limitation for this approach. On the other hand, cellular encapsulation is a new strategy to provide immune isolation to avoid host rejection of grafts. Among the current existing techniques, microencapsulation entails several benefits: it allows the encapsulation of single islets by generation of spherical gels of micrometric size and with optimal surface / volume ratio, as compared to macroencapsulation systems [19]. Microcapsules indeed facilitate a rapid exchange of oxygen, glucose, insulin and nutrients between the capsule and the environment [19]. One of the most used biomaterials for encapsulation is sodium alginate, a natural copolymer that changes its physical state, from liquid to gel, in presence of divalent cations (mainly Ba^{2+} or Ca^{2+}) [19]. It has been reported that encapsulation of islets in Ba^{2+} -alginate preserve islet function *in vitro* with similar regulated insulin secretion compared to non-encapsulated islets [19]. In addition, Safley et al. demonstrated *in vivo* biocompatibility of Ba^{2+} -alginate microgels [20], and others *in vivo* studies have demonstrated that Ba^{2+} -alginate microgels provide long term immunoprotection in animal models [21, 22, 23]. In previous studies, successful allotransplant of parathyroid tissue encapsulated in Ba^{2+} -alginate was reported in a patient suffering of severe hypocalcemia due to an iatrogenic parathyroid resection. In this case, the grafted tissue showed functionality for at least 20 months with a mild requirement of oral calcium supplementation [24, 25]. Considering this same principle, we hypothesized that we could generate functional, microencapsulated IPC/GPC aggregates *in vitro*, from IPC and GPC differentiated from hASC.

2. Materials And Methods.

2.1 Isolation and Cell Culture of hASC.

This study was approved by the Research Ethics Committee, Faculty of Medicine, University of Chile. Adipose tissue was obtained from five donors aged between 30 and 45 years undergoing abdominal liposuction cosmetic surgery. Informed consent was obtained from all participants. hASC were obtained from lipoaspirated fat tissue, the tissue was digested by type I collagenase 0,2% p/v (Worthington, NJ, USA. Catalog number LS004196) and the stromal vascular fraction (SVF) was cultured in DMEM:F12 1:1 (Gibco™, Dublin, Irlanda. Catalog number 12500062) medium supplemented with 10% fetal bovine serum (FBS), denominated supplemented medium, at 37°C and 5.0% CO₂.

2.2 Differentiation to IPC from hASC *in vitro*.

hASC were differentiated *in vitro* to IPC using a two-stage protocol, [13, 14], with discrete modifications. Cells were stimulated for 7 days with DMEM high glucose (25 mM) (Gibco™, Dublin, Irlanda. Catalog number 12100046); followed by 14 days with DMEM low glucose (5 mM) (Gibco™, Dublin, Irlanda. Catalog number 31600034). Both media were supplemented with 2 nM activin A (Prospecbio, CA, USA. Catalog number CYT-145), 10 mM nicotinamide (Sigma-Aldrich, Merck KGaA, Darmstadt, Germany. Catalog number N0636) and 10 nM glucagon like peptide (GLP-1) (Prospecbio, CA, USA. Catalog number HOR-284). However, we used 2% FBS instead of 10% as a supplement to differentiation medium during all differentiation, **Figure 1A**.

2.3 Differentiation to GPC from hASC *in vitro*. GPC were obtained by the protocol reported for Rezanian et al. [15] with modifications. The protocol consists in 6 stages: stage 1, incubated for 4 days with RPMI 1640 (Gibco™. Catalog number 31800), bovine serum albumin (BSA) (Sigma-Aldrich, catalog number A9418) 2%, activin A 100 ng/mL (Prospecbio), Wnt3a 20 ng/mL (Sigma-Aldrich. Catalog number H17001), FGF2 8 ng/mL (Prospecbio. Catalog number CYT-085). Stage 2, incubated for 2 days with DMEM-F12 medium with BSA 2%, FGF7 50 ng/mL (Prospecbio. Catalog number CYT-303), Cyclopamine-KAAD 0,25 µM (SCBT, Dallas, Tx, USA. Catalog number sc-200929). Stage 3, incubation for 4 days with DMEM-F12 medium, Cyclopamin-KAAD 0,25 µM, retinoic acid (RA) 2 µM (Sigma-Aldrich. Catalog number R2625), FGF7 50 ng/mL (Prospecbio), Noggin 100 ng/mL (Prospecbio. Catalog number CYT-475). Stage 4, incubation for 3 days with DMEM:F12 medium, Inhibitor II ALK5 1 µM (SCBT. Catalog number sc-221234), Noggin 100 ng/mL, DAPT 1 µM (SCBT. Catalog number sc-201315). Stage 5, incubation for 7 days with DMEM/F12 medium, inhibitor II ALK5 1 µM. Stage 6, incubation for 7 days with DMEM F12 medium. However, we used 2% FBS instead of 1% B27 as a supplement to differentiation medium during stages 3 to 6, **Figure 1B**. **2.4 Formation of cell aggregates.** The formation of cells aggregates was induced applying a proprietary protocol that subjects cell to low adherence conditions and progressive clustering, as previously described [26]. Briefly, differentiated IPC and GPC cells were incubated in a 4:1 ratio respectively, using 10⁵ total cells, under conditions of non-adherence. This protocol combines 1) the use of bacteriological plates with low electrical charge, and 2) culturing in low Ca²⁺ and Mg²⁺ using a special

formulation of Eagle Minimum Essential Medium, Joklik Modification (Sigma-Aldrich. Catalog number M0518) and 3) reduced concentration of FBS (2% v/v) for up to 7 days.

2.5 Immunofluorescent staining.

2.5.1 Immunofluorescence of adherent cells.

Undifferentiated and differentiated cells were grown in glass coverslips and fixed for 10 min with 4% paraformaldehyde (PFA) (Sigma-Aldrich. Catalog number 158127) in phosphate buffer saline (PBS) at room temperature, washed, and then permeabilized with 0.3% triton X-100 (Sigma-Aldrich. Catalog number T8787) for 10 min and incubated with 3% BSA in PBS (to block non-specific binding) for 45 min. Cells were then incubated overnight at 4°C with Abcam primary antibodies (Abcam, Cambridge, UK) (Ms anti-C44 catalog number ab6124, Goat anti-Pdx1 catalog number ab47383, Rb anti-Ngn3 catalog number ab38548, GPig anti-Ins catalog number ab7842, Mouse anti-Gcg catalog number ab 10988, and Goat anti-Vim catalog number V-4630 (Sigma-Aldrich). Cells were then washed with PBS and incubated with corresponding secondary antibodies for 90 min at RT (Dnk anti-mouse catalog number ab96875, Dnk anti-goat catalog number ab96933, Dnk anti-rb catalog number ab96919, Dnk anti-GPig catalog number ab150185, Goat anti-mouse catalog number ab6787, Dnk anti-goat catalog number ab96931) (Abcam). Cells were washed with PBS and then incubated with Hoechst (Millipore, Massachusetts, USA) 1:500 for 5 min at RT. Covers were washed and mounted in slides with fluorescence mounting medium DAKO (Agilent, CA, USA. Catalog number S302380). The images were analyzed using confocal microscopy (LSM700, Zeiss) and the ImageJ public domain software.

2.5.2 Immunofluorescence of cell aggregates.

Prior to immunofluorescence, cell aggregates formed after 72 h were fixed in 4% PFA for 1 hour and added to 1% liquid low melting agarose (Sigma-Aldrich, catalog number A9414) in PBS (50°C). To obtain cell blocks, the agarose-cell mix was centrifuged at 1500 rpm for 5 min at RT. Cryostat sections of 6 µm were submitted to conventional IFI and visualized by confocal microscopy (LSM 700, Carl Zeiss).

2.6 ELISA assay. To test if the hormonal release of IPC, GPC cells and aggregates was glucose-dependent, two glucose concentrations (2 mM and 25 mM) were assayed. After pre-incubation with Krebs-Ringer buffer (KRB) without glucose (120 mM NaCl, 5 mM KCl, 2,5 mM CaCl₂, 1,1 mM MgCl₂, 25 mM NaHCO₃, 10 mM HEPES, 0.1 % BSA) at 37°C for 2 h, the cells were incubated with KRB containing 2 mM glucose at 37°C for 4 h. To induce insulin release, the cells were incubated with KRB containing 25

mM glucose for another 4 h. Then, the respective conditioned media were collected and tested for the content of released insulin with human insulin (Merckodia, Uppsala, Sweden. Catalog number 10-1132-01) and human glucagon (Cusabio, Houston, TX, USA. Catalog number CSB-E09207h) ELISA kits

2.7 Microencapsulation of cell aggregates. Alginate microgels were automatically produced using the dripping technique. As a polymer, 1,5% (MW medium) sodium alginate (Sigma- Aldrich. Catalog number A2033) dissolved in 0,9% NaCl was used. The stabilizing solutions of calcium and barium chloride was maintained at pH 7.0 and was composed of (in mM): BaCl₂ (20), NaCl (115), and histidine (50), or CaCl₂ (40), NaCl (85), HEPES (10). First, 1 mL of sodium alginate solution (1,5% w/v) was mixed with 20⁴ cellular aggregates previously filtered through 40 µm and 120 µm sieves. This anionic suspension was pumped using a Microencapsulator B-395Pro (Büchi, Flawil, Switzerland), equipped with a 150 µm nozzle over a stirring barium or calcium chloride solution for 30 seconds, with a dripping flow of 32 mL/min, 3000 Hz frequency and 1000 V voltage, as previously reported [27, 28]. After its formation, the microgels were washed with 0.9% NaCl and incubated in DMEM / F12 medium supplemented with 10% FBS in cell culture conditions (37 °C, 5.0% CO₂). Additionally, rupture of the microgels was evaluated by dissolving the alginate with a solution composed of solution composed of 100 mM sodium citrate, 10 mM MOPS and 27 mM NaCl according to reports from Wang et al. [29].

2.8 Statistical analysis. For the experiments of cell aggregate formation and encapsulation of BSA or SpA proteins, statistical analysis was performed using one-way ANOVA followed by Student's *t* test as post-hoc. Student *t* test was used in Ins or Gcg release tests. Differences were deemed statistically significant for p-values of less than 0.05.

3. Results.

3.1 Characterization of hASC.

The SVF obtained from each patient was used as a source of MSC, denominated hASC, and characterized following the mesenchymal stem cell minimal criteria described by Dominici et al. [30]. To define these cells as a population of hASC, we validated the specific pattern of surface markers associated to these cells by flow cytometry (**Table S1**). The results of hASC characterization obtained from 5 donors confirmed that these cells were positive for expression of CD90, CD73, CD105, CD44, and CD29, while lacking expression of CD45, CD34, CD19 and HLA-DR surface markers. Moreover, we tested the differentiation potential of these cells to adipogenic, osteogenic and chondrogenic phenotype, and confirmed that hASC were able to differentiate to these three lineages compared to undifferentiated hASC, as evidenced by the detection of known characteristic features of differentiation such as the

presence of lipidic intracellular vacuoles in adipogenic cells, calcium deposition determined by Von Kossa staining in osteogenic cells; and finally, sulfated mucines detected by alcian blue staining in chondrogenic cells (**Figure S1**).

3.2 Generation and characterization of IPC and GPC. After application of the in vitro differentiation protocol, we performed immunofluorescence analysis in IPC and GPC, which showed presence and nuclear localization of β cell specific transcription factors as Pdx1 and Ngn3, **Figure 2**. On the other hand, hASC, expressed these markers poorly, with diffuse distribution (**Figure 2A**). Moreover, IPC expressed insulin, which was not evident in hASC, (**Figure 2B**). Further, insulin secretion by IPC treated with external high glucose (25mM) increased 5-fold compared to undifferentiated cells (**Figure 3A**). Conversely, GPC cells express glucagon and secrete the hormone in response to low glucose concentration in the medium 4-fold greater than undifferentiated cells, **Figure 3B**. These results suggest that our differentiation protocol of hASC to IPC and GPC, strongly reproduce the functionality of these cells.

3.3 Cell aggregate formation.

The results of IPC/GPC aggregate formation over time is shown in **Figure 4A**. At 24 h of culture, aggregates are not yet evident. However, at 48 h almost all cells are aggregated. At 72 y 96 h, these formations were significantly larger. Finally, at day 7, the aggregates tend to lose their shape and cellular debris appears, suggesting cell death. The analysis by optical microscopy reveals that the area of the aggregates increased in time, **Figure 4B**. At 24 h, we estimated that 55% of the aggregates have an area below $2000 \mu\text{m}^2$. At 48 h, most aggregates (65%) reached at least $2500 \mu\text{m}^2$. At 72 and 96 h, 65 % of the aggregates reached $4000 \mu\text{m}^2$. By day 7, all aggregates comprised areas from 1000 and $4000 \mu\text{m}^2$, suggesting a slow decay of the aggregate structure at this time. Later, cell aggregates incubated at different times were filtered through $40\mu\text{m}$ and $120\mu\text{m}$ sieves to concentrate the aggregates within these sizes and evaluate the best time to obtain larger aggregates in a stable manner. When calculating the diameter, we found that at 72 h, most aggregates had similar diameters ($\sim 80 \mu\text{m}$), **Figure 4C**. Finally, confocal microscopy studies in cryostat sections of differentiated cell aggregates revealed the presence of Insulin and Pdx1, and very faint staining for glucagon (**Figure 5**).

3.4 Microcapsules of cell aggregates.

The aggregates were encapsulated in sodium alginate stabilized by Ca^{2+} o Ba^{2+} cations. Detection of alginate particle diameters by optical microscopy indicated that microgels generated were spherical, with an approximate diameter of $\sim 310 \mu\text{m}$ (**Figure 6A and Table 1**). To evaluate the permeability of microgels, SpA and BSA proteins (40 and 60 kDa, respectively) were previously encapsulated in 1,5% sodium

alginate and stabilized by Ca^{2+} or Ba^{2+} cations, see Supplemental information. These microgels presented sizes similar (**Table S2**) to those used to encapsulate cellular aggregates (**Table 1**). When then evaluated the encapsulation efficiency of our alginate microcapsules, which was estimated to be in the 54 and 58% range, that is, 54 to 58% of the total protein was encapsulated, whereas 46 to 42% of the protein remained in the stabilization medium without being incorporated into the microgel. No significant differences were found between encapsulated BSA or SpA proteins, (**Figure S2**).

Interestingly, when determining the release of SpA or BSA from the microgels to KRB, we observed a burst effect achieving up to of 13% of release in the first 5 minutes of incubation in both, Ca^{2+} or Ba^{2+} stabilized cations, (**Figure S2**). Then a steady state is reached at 15 and 20 min where achieving up to 16% of protein release in both, Ca^{2+} or Ba^{2+} microgels (**Figure S2**), without finding significant differences between microgels formed with Ca^{2+} or Ba^{2+} , nor between microgels containing SpA protein or BSA.

IPC/GPC cellular aggregates encapsulation, we observed that cell aggregates microencapsulated in Ca^{2+} did not adequately stabilize alginate microgels, which began to swell and degrade after 96 h in culture conditions. Conversely, Ba^{2+} stabilized microgels were stable after 7 days, (**Figure 6A**). IPC/GPC Ba^{2+} stabilized microgels, were capable of secreting insulin in response to elevated glucose concentrations (HG, 25 mM) at 1 day, (**Figure 6B**). However, after 7 days *in vitro*, this response decayed, and no significant differences were found with respect to control (**Figure 6C**).

4. Discussion.

Differentiation to IPC can be achieved from various cellular sources such as: embryonic stem cells (ESC) [31], induced pluripotent stem cells (iPSCs) [32] and MSC derived from adult tissue, as adipose (hASC) [13] [14], bone marrow (BM-MSC), [33] dental pulp (DPSCs) [34], and placenta [34]. Use of ESC and iPSCs in clinic is not routinely approved due to ethics and implementation considerations. Yet, hASC can be easily obtained from low invasive lipoaspiration procedures with high yield of cell purification. Hence, these cells constitute an important source of MSC [11, 12].

The hASC obtained in this work meet the requirements dictated by the International Society of Cell Therapy (ISCT) to classify a cellular population as a MSC [27, 35, 36]. Our cells were able to adhere to plastic with a fibroblastic phenotype, they expressed CD90, CD73, CD105, CD44, and CD29 while lacking expression of CD45, CD34, CD19 and HLA-DR, concordant to the surface marker expression described for hASC [11, 12]. Moreover, they were able to differentiate to adipogenic, chondrogenic and osteogenic phenotypes.

We then established a reliable method to induce differentiation of this cells into both IPC and GPC *in vitro*. Our results agree with those of other groups, in particular the differentiation process of hASC to IPC, [13, 14]. On the other hand, differentiation to GPC have only been reported from ESC [15]. To the best of our knowledge, we are the first group to achieve an efficient and functional GPC differentiation from hASC using the protocol described by Rezanian group, yet using SFB 2 % instead of the B27 supplement.

For GPC differentiation, we decided to use 2% FBS instead of 1% B27 as a supplement in the differentiation medium during stages 3 to 6 (Figure 1B), a modification reached empirically, which provided more effective differentiation and greater survival, and it also matched the serum concentration used in our subsequent aggregation protocol. In line with these findings, we propose hASC as an adequate cellular source to generate IPC and GPC in cell-based therapy against T1DM.

Next, we co-cultured IPC and GPC in a 4:1 ratio by inducing cellular aggregation in low adhesion conditions, as previously described [26]. Using this setting, we observed that cell aggregates increased in size up to 72 h, reaching diameters of $\sim 80 \mu\text{m}$, similar to those reported for human islets ($108 \mu\text{m}$) [37]. Expression of α and β pancreatic cell markers in 72 h old cellular aggregates was also conserved, indicating a strong lineage commitment and low dedifferentiation rate of our cells.

Although human like islets should be able to partially restore the pancreatic endocrine function, the activation of the immune system is still a major limitation, together with the low number of donors for long term treatment [6, 8]. To overcome this issue, we encapsulated our IPC/GPC aggregates into sodium alginate microgels using an automatized encapsulator. The size of Ca^{2+} or Ba^{2+} stabilized sodium alginate microgels pools were very similar, with very low dispersion. In culture conditions, Ca^{2+} stabilized microgels increased in size and were less stable than Ba^{2+} stabilized microgels, which maintained their size and shape even after 7 days of culture. An explanation to this phenomenon lies in the chemical characteristics of the sodium alginate copolymer, which is composed by 1,4-b-D-mannuronic acid (M) and 1,4-a-L-guluronic acid (G) residues, and can be stabilized in general terms by divalent cations being Ba^{2+} the most efficient ($\text{Mg}^{2+} \ll \text{Ca}^{2+} < \text{Sr}^{2+} < \text{Ba}^{2+}$) [19].

Several studies have aimed to improve the output of encapsulated tissue grafts using sodium alginate. However, variables such as alginate purity and immunological response against residual contaminants left from the purification process are still a matter of discussion, [19]. In our setting, both Ca^{2+} or Ba^{2+} stabilized alginate microgels were able to release both BSA and SpA proteins in the first 5 minutes, yet after 20 minutes the release rate diminished and remained stable. This information defined the alginate microgels pore size, which in essence permits the passage of nutrient such as glucose, as well as small peptides as Ins and Ggc. In agreement with these findings, we also confirmed that our microencapsulated cellular aggregates responded to external glucose by secreting Ins, thus confirming that the microgels allowed the passage of glucose into the microgel to be sensed by the cellular aggregates, which in turn responded by secreting insulin. Also, we observed that undifferentiated hASCs do exhibit a small secretion of insulin in response to external glucose stimulation, which is agreeable with previous reports that explain such phenomena as a result of possible basal, spontaneous differentiation, both in adherent as well as in suspension conditions [38]. It is therefore possible that a small percentage of cells kept in control conditions could have spontaneously differentiated into a pancreatic endocrine phenotype.

Despite the stability of the microgels, IPC/GPC aggregates ceased to secrete insulin after 7 days in culture. This may be attributable to loss of β cell function due to a dedifferentiation process, a desensitization of the IPC to glucose, or poor survival of the cellular aggregate in encapsulation

conditions in the *in vitro* environment. Indeed, the described differentiation protocols attempted to reproduce the embryogenic process observed in organs and tissues *in vitro*. Yet the complexity of the embryogenic process in cell differentiation differs substantially from the much simpler *in vitro* milieu, a situation that could result in dedifferentiation, and in turn loss of phenotypic and functional characteristics. Nevertheless, an *in vivo* environment may overcome such limitations. We are currently planning experiments with *in vivo* implantation of our encapsulated clusters in NOD mice, an animal model of T1DM, which may shed light on this issue.

Our findings enforce the current knowledge on the potential of hASC as a source of multipotent cells in cellular therapy against T1DM. Moreover, we have developed a protocol to generate functional aggregates IPC/GPC like pancreatic islets, which can be encapsulated in alginate microgels to achieve immunoprotection. In such conditions, the encapsulated aggregates are stable and retain endocrine function *in vitro* for at least 7 days in culture.

3. Conclusions.

In the present work, we have achieved *in vitro* functional differentiation of human multipotent stem cells to IPCs and GPCs. Indeed, we have effectively attained IPCs and GPCs coaggregation to form islet-like clusters, and subsequently microencapsulation in alginate. Cell aggregates retain the capability of expressing endocrine pancreatic markers. Microencapsulation was standardized using a sterile, automated and highly reproducible procedure, thus optimizing protection from eventual immunological rejection after implants. Further, the microcapsules are capable of secreting insulin when subjected to external glucose stimulation.

Finally, the cell coaggregate formation conditions reported herein provide the basis for aggregation of any cell type, projecting its use in other pathologies where replacement of cell mass or function is required. Also, our findings may give rise to new studies, where the functionality of microgels and aggregates can be evaluated *in vivo*. In this way, the proposed therapy would, on the one hand, immunologically isolate cellular aggregates and, secondly, avoid immunosuppressive treatment.

Declarations

Ethics approval and consent to participate

The Ethics Committee for research in human of the Faculty of Medicine, University of Chile, approved this project under # 033-2014, according to the directives of the Helsinki Declaration concerning human rights. Donors consented freely to donate fat tissue for the present study.

Consent for publication

All authors have reviewed and approved this manuscript, and are aware it is being submitted for publication.

Availability of data and materials

All data generated or analyzed during this study are included in this published article and enclosed supplementary information files.

Competing interests.

Pablo Caviedes holds patent protection on the cell aggregation protocol. The remaining authors declare no conflict of interests.

Funding.

- Claudia Jara, PhD National Scholarship grant, # Conicyt, Chile.
- Felipe Oyarzún, FONDECYT 1161450, FONDEQUIP EQM160157, FONDEQUIP EQM170111, CONICYT-FONDAP 15130011. FONDECYT 1201899, ANID/PIA/ACT192144.
- Flavio Carrion: Fondecyt 1130444.
- Pablo Caviedes, FONDECYT grant # 1130241,1161450, CONICYT for funding of Basal Centre, CeBiB, FB0001 and P09-022-F from ICM-ECONOMIA, Chile.

Authors' contributions

Claudia Jara designed and performed most of the experiments and writing of this manuscript. Felipe Oyarzun-Ampuero provided access to the microencapsulator and feedback on establishing the conditions for microencapsulation of cell clusters and writing of this manuscript. Flavio Carrión provided access to flow cytometry studies and necessary input on mesenchymal cell characterizations, as well as writing of this manuscript. Esteban González-Echeverría carried out lipoaspiration procedures and first manipulations of tissue samples and provided input in writing this manuscript. Claudio Cappelli provided valuable input in writing this manuscript. Pablo Caviedes provided input in all aspects of this work, as well as tutoring Claudia Jara in her work, and in writing this manuscript.

Acknowledgements

The authors acknowledge the invaluable technical assistance of Mr. Fernando Guzmán and Mr. Guillermo Elorza.

References

1. Ize-Ludlow D., Sperling MA. The classification of diabetes mellitus: a conceptual framework. *Pediatr Clin N Am.* 2005, 52(6): 1533-1552. doi:10.1016/j.pcl.2005.07.001.
2. Rutter, GA. and Hodson, DJ. Minireview: intraislet regulation of insulin secretion in humans. *Mol Endocrinol.* 2013, 27(12): 1984–1995. doi:10.1210/me.2013-1278.
3. Shapiro AM, Ricordi C, Hering BJ, et al. International trial of the Edmonton protocol for islet transplantation. *N Engl J Med.* 2006, 355(13):1318-1330. doi:10.1056/NEJMoa061267.
4. Shapiro AM, Lakey JR, Ryan EA, et al. Islet Transplantation in Seven Patients with Type 1 Diabetes Mellitus Using a Glucocorticoid-Free Immunosuppressive Regimen. *N Engl J Med.* 2000;343(4):230-238. doi:10.1056/NEJM200007273430401.
5. Ryan EA, Lakey JR, Rajotte RV, et al. Clinical outcomes and insulin secretion after islet transplantation with the Edmonton protocol. *Diabetes* 2001, 50(4):710–719. doi:10.2337/diabetes.50.4.710.
6. Ryan EA, Paty BW, Senior PA, Shapiro AM. Risks and side effects of islet transplantation. *Curr Diab Rep.* 2004;4(4):304-309. doi:10.1007/s11892-004-0083-8
7. Vincenti F, Friman S, Scheuermann E, et al. Results of an international, randomized trial comparing glucose metabolism disorders and outcome with cyclosporine versus tacrolimus. [published correction appears in *Am J Transplant.* 2008 Apr;8(4):908. Dosage error in article text] [published correction appears in *Am J Transplant.* 2008 Jan;8(1):1]. *Am J Transplant.* 2007, 7(6):1506-1514. doi:10.1111/j.1600-6143.2007.01749.x
8. Ichii, H., Ricordi, C. Current status of islet cell transplantation. *J Hepatobiliary Pancreat Surg.* 2009; 16(2):101-112. doi:10.1007/s00534-008-0021-2.
9. Matsumoto S, Abalovich A, Wechsler C, Wynyard S, Elliott RB. Clinical Benefit of Islet Xenotransplantation for the Treatment of Type 1 Diabetes. *EBioMedicine.* 2016; 12:255-262. doi:10.1016/j.ebiom.2016.08.034.
10. da Silva Meirelles L, Chagastelles PC, Nardi NB. Mesenchymal stem cells reside in virtually all post-natal organs and tissues. *J. Cell Sci.* 2006, 119(Pt 11): 2204–2213. doi:10.1242/jcs.02932
11. Kern S, Eichler H, Stoeve J, Klüter H, Bieback K. Comparative analysis of mesenchymal stem cells from bone marrow, umbilical cord blood, or adipose tissue. *Stem cells.* 2006; 24(5): 1294-1301. doi:10.1634/stemcells.2005-0342.
12. Heo JS, Choi Y, Kim HS, Kim HO. Comparison of molecular profiles of human mesenchymal stem cells derived from bone marrow, umbilical cord blood, placenta and adipose tissue. *Int J Mol Med.* 2016; 37(1):115-25. doi:10.3892/ijmm.2015.2413.
13. Mohamad Buang ML, Seng HK, Chung LH, Saim AB, Idrus RB. In vitro generation of functional insulin-producing cells from lipoaspirated human adipose tissue-derived stem cells. *Arch Med Res.* 2012; 43(1): 83-88. doi:10.1016/j.arcmed.2012.01.012.
14. Kang HM, Kim J, Park S, et al. Insulin-secreting cells from human eyelid-derived stem cells alleviate type I diabetes in immunocompetent mice. *Stem Cells.* 2009; 27(8):1999-2008. doi:10.1002/stem.127.

15. Rezanian A, Riedel MJ, Wideman RD, et al. Production of functional glucagon-secreting α -cells from human embryonic stem cells. *Diabetes*. 2011; 60 (1), 239-247. doi:10.2337/db10-0573.
16. Timper K, Seboek D, Eberhardt M, et al. Human adipose tissue-derived mesenchymal stem cells differentiate into insulin, somatostatin, and glucagon expressing cells. *Biochem Biophys Res Commun*. 2006; 341(4), 1135-1140. doi:10.1016/j.bbrc.2006.01.072.
17. Chandra V, Swetha G, Muthyala S, et al. Islet-like cell aggregates generated from human adipose tissue derived stem cells ameliorate experimental diabetes in mice. *PLoS One*. 2011; 6(6):e20615. doi: 10.1371/journal.pone.0020615.
18. Watts M, Ha J, Kimchi O, Sherman A. Paracrine regulation of glucagon secretion: the $\beta/\alpha/\delta$ model. *Am J Physiol Endocrinol Metab*. 2016;310(8):E597-E611. doi:10.1152/ajpendo.00415.2015.
19. Paredes Juárez GA, Spasojevic M, Faas MM, de Vos P. Immunological and technical considerations in application of alginate-based microencapsulation systems. *Front Bioeng Biotechnol*. 2014;2:26. doi:10.3389/fbioe.2014.00026;
20. Safley SA, Cui H, Cauffiel S, Tucker-Burden C, Weber CJ. Biocompatibility and immune acceptance of adult porcine islets transplanted intraperitoneally in diabetic NOD mice in calcium alginate poly-L-lysine microcapsules versus barium alginate microcapsules without poly-L-lysine. *J Diabetes Sci Technol*. 2008;2(5):760-767. doi:10.1177/193229680800200503.
21. Schneider S, Feilen PJ, Brunnenmeier F, et al. Long-term graft function of adult rat and human islets encapsulated in novel alginate-based microcapsules after transplantation in immunocompetent diabetic mice. *Diabetes*. 2005;54(3):687-693. doi:10.2337/diabetes.54.3.687.
22. Omer A, Duvivier-Kali V, Fernandes J, Tchpashvili V, Colton CK, Weir GC. Long-term normoglycemia in rats receiving transplants with encapsulated islets. *Transplantation*. 2005;79(1):52-58. doi:10.1097/01.tp.0000149340.37865.46.
23. Qi M, Strand BL, Mørch Y, et al. Encapsulation of human islets in novel inhomogeneous alginate- Ca^{2+}/Ba^{2+} microbeads: in vitro and in vivo function. *Artif Cells Blood Substit Immobil Biotechnol*. 2008; 36(5):403-402. doi:10.1080/10731190802369755.
24. Cabané P, Gac P, Amat J, et al. Allograft of microencapsulated parathyroid tissue in severe postsurgical hypoparathyroidism: a case report. *Transplant Proc*. 2009;41(9):3879-3883. doi:10.1016/j.transproceed.2009.06.211.
25. Toledo PC, Rossi RL, Caviedes P. Microencapsulation of Parathyroid Cells for the Treatment of Hypoparathyroidism. *Methods Mol Biol*. 2017; 1479:357-363. doi: 10.1007/978-1-4939-6364-5_27.
26. Caviedes P, Caviedes R, Freeman T, et al. 2008. Pub US Patent No 7323333 B2.
27. Hassan N, Oyarzun-Ampuero F, Lara P, Guerrero S, Cabuil V, Abou-Hassan A, Kogan M.J. Flow Chemistry to Control the Synthesis of Nano and Microparticles for Biomedical Applications. *Curr Top Med Chem*. 2014 Mar;14(5):676-89. doi:10.2174/1568026614666140118213915.
28. Inostroza-Riquelme M, Vivanco A, Lara P, Guerrero S, Salas-Huenuleo E, Chamorro A, Leyton L, Bolaños K, Araya E, Quest A.F.G, Kogan M.J., Oyarzun-Ampuero F. Encapsulation of Gold

- Nanostructures and Oil-in-Water Nanocarriers in Microgels With Biomedical Potential. *Molecules*. 2018 May 18;23(5):1208. doi: 10.3390/molecules23051208.
29. Wang N, Adams G, Buttery L, Falcone FH, Stolnik S. Alginate encapsulation technology supports embryonic stem cells differentiation into insulin-producing cells. *J Biotechnol*. 2009;144(4):304-312. doi:10.1016/j.jbiotec.2009.08.008.
 30. Dominici M, Le Blanc K, Mueller I, et al. Minimal criteria for defining multipotent mesenchymal stromal cells. The International Society for Cellular Therapy position statement. *Cytotherapy*. 2006, 8(4):315-7. doi:10.1080/14653240600855905.
 31. Hua XF, Wang YW, Tang YX, et al. Pancreatic insulin-producing cells differentiated from human embryonic stem cells correct hyperglycemia in SCID/NOD mice, an animal model of diabetes. *PLoS One*. 2014;9(7):e102198. doi:10.1371/journal.pone.0102198.
 32. Jeon K, Lim H, Kim JH, et al. Differentiation and transplantation of functional pancreatic beta cells generated from induced pluripotent stem cells derived from a type 1 diabetes mouse model. *Stem Cells Dev*. 2012;21(14):2642-2655. doi:10.1089/scd.2011.0665
 33. Gabr MM, Zakaria MM, Refaie AF, et al. Insulin-producing cells from adult human bone marrow mesenchymal stem cells control streptozotocin-induced diabetes in nude mice. *Cell Transplant*. 2013, 22(1):133-145. doi:10.3727/096368912X647162.
 34. Carnevale G, Riccio M, Pisciotta A, et al. In vitro differentiation into insulin-producing β -cells of stem cells isolated from human amniotic fluid and dental pulp. *Dig Liver Dis*. 2013, 45(8):669-76.
 35. González E, Carrión F, Caviedes P. The UCHT1 method have a proliferative effect in human adipose stem cells (hASC), in 1st National Congress of Tissue Engineering and Regenerative Medicine, LAP LAMBERT Academic Publishing, 2018, p. 77-79, Mauritius, ISBN: 978-613-3-99514-7.
 36. Bourin P, Bunnell BA, Casteilla L, et al. Stromal cells from the adipose tissue-derived stromal vascular fraction and culture expanded adipose tissue-derived stromal/stem cells: a joint statement of the International Federation for Adipose Therapeutics and Science (IFATS) and the International Society for Cellular Therapy (ISCT). *Cytotherapy*. 2013; 15(6):641-8. doi:10.1016/j.jcyt.2013.02.006.
 37. Ionescu-Tirgoviste C, Gagniuc PA, Gubceac E, et al. A 3D map of the islet routes throughout the healthy human pancreas. *Sci. Rep*. 2015; 5: 14634. doi:10.1038/srep14634.
 38. Assady S, Maor G, Amit M, Itskovitz-Eldor J, Skorecki KL, and Tzukerman M. Insulin Production by Human Embryonic Stem Cells. *Diabetes* 2001;50(8):1691–1697. doi:10.2337/diabetes.50.8.1691.

Tables

Sample	Diameter, time 0 (µm)		Diameter 7 days (µm)	
	CaCl ₂	BaCl ₂	CaCl ₂	BaCl ₂
Alginate 1,5%-hASC aggregate	310 ± 14	303 ± 23	459 ± 28 *	314 ± 15
Alginate 1,5%-IPC/GPC aggregate	302 ± 13	309 ± 12	468 ± 27 *	316 ± 9

Table 1: Diameter of microencapsulated cell aggregates in 1.5% sodium alginate. Sizes

of microgels were analysed by ImageJ in at least 10 photographs for each n, n=3, *p<0,05.

Figures

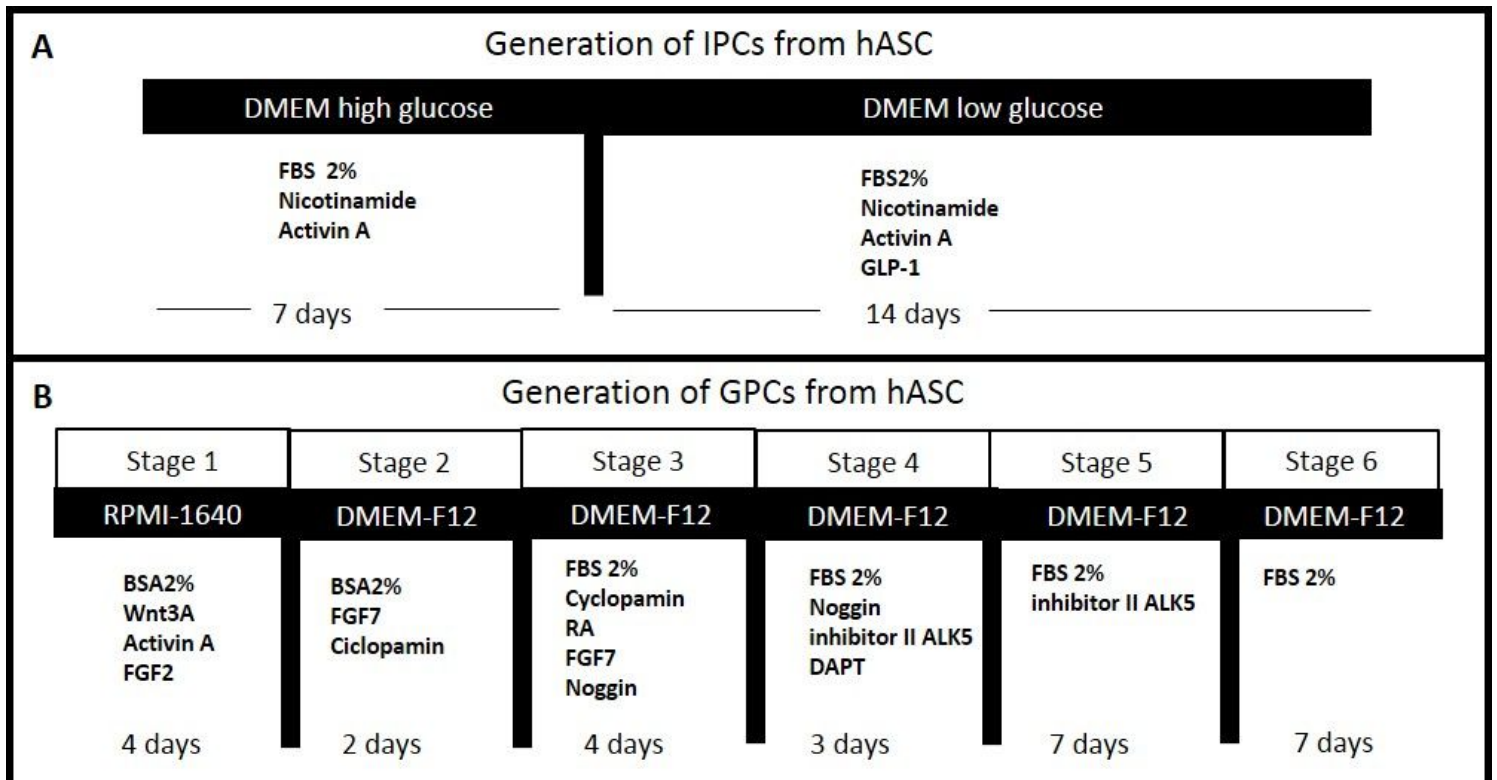


Figure 1

Schematic representation of differentiation protocols from hASC to IPC and GPC. A) IPC differentiation protocol in two stages during 21 days. B) CPG differentiation protocol in 6 stages during 27 days. FBS: fetal bovine serum, GLP-1: glucagon like-peptide 1, BSA: Bovine serum albumin, FGF2: fibroblastic growth factor 2, RA: retimoic acid, FGF7: fibroblastic growth factor 7, ALK 5: TGFβ type I receptor kinase, DAPT: Gamma-Secretase Inhibitor IX (N-[N-(3,5-Difluorophenacetyl-L-alanyl)]-S-phenylglycine t-butyl ester).

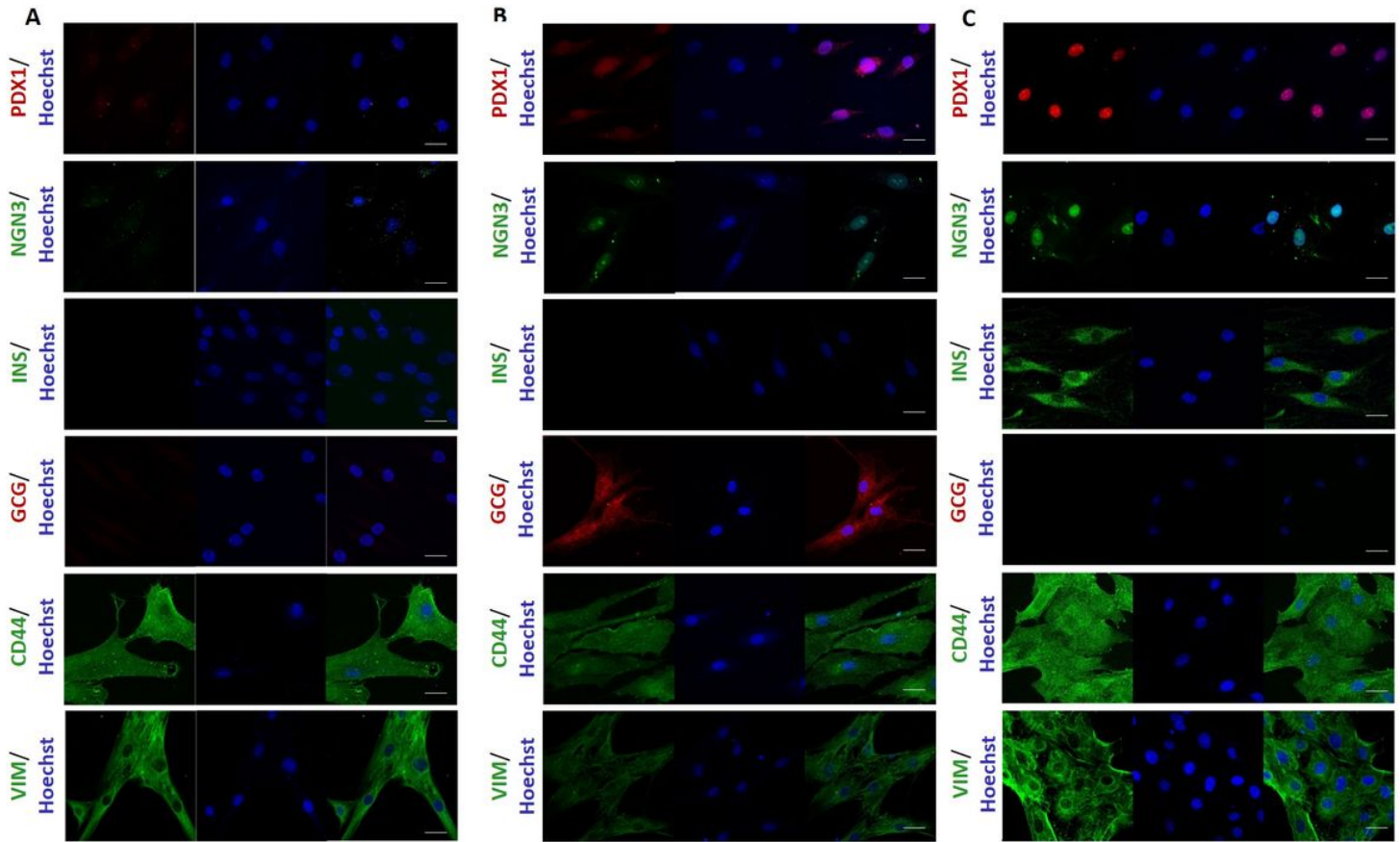


Figure 2

Expression of differentiation markers in hASC, IPC and GPC by indirect immunofluorescence. The images shown are representative of n=3 experiments, visualized by confocal microscopy. Nuclear staining was performed with Hoechst 1: 500 (blue). Markers analyzed were Pdx1 (red), Ngn3 (green), Insulin (green), Glucagon (red), CD44 (green) and Vimentin (green). A) Markers analyzed in hASC. B) Markers analyzed in IPC. C) Markers analyzed in GPC. Scale bar= 20 μ m. Pdx1: pancreatic and duodenal homeobox 1, Ngn3: neurogenin 3, Ins: insulin, Gcg: glucagon, Vim: vimentin.

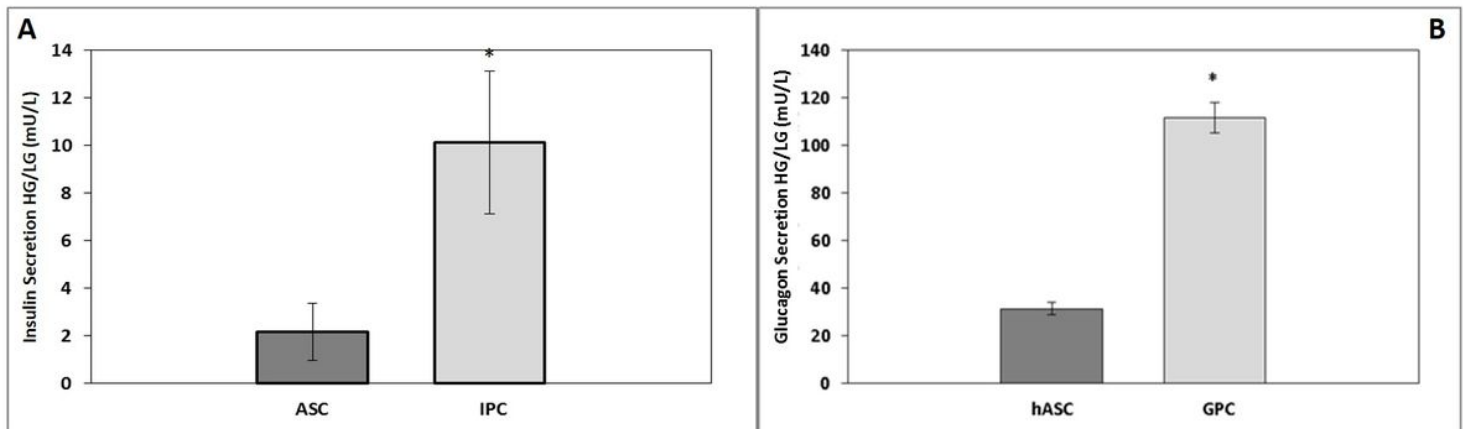


Figure 3

Hormonal secretion in response to low or high external glucose concentration in vitro. Glucose challenge was performed by incubating the cells with low-glucose buffer (2mM) or high-glucose buffer (25 mM) for 4h. A) Insulin secretion in response to high glucose in vitro. B) Glucagon secretion in response to low glucose in vitro. n=3. * Significant $p < 0.05$ (Student's t test).

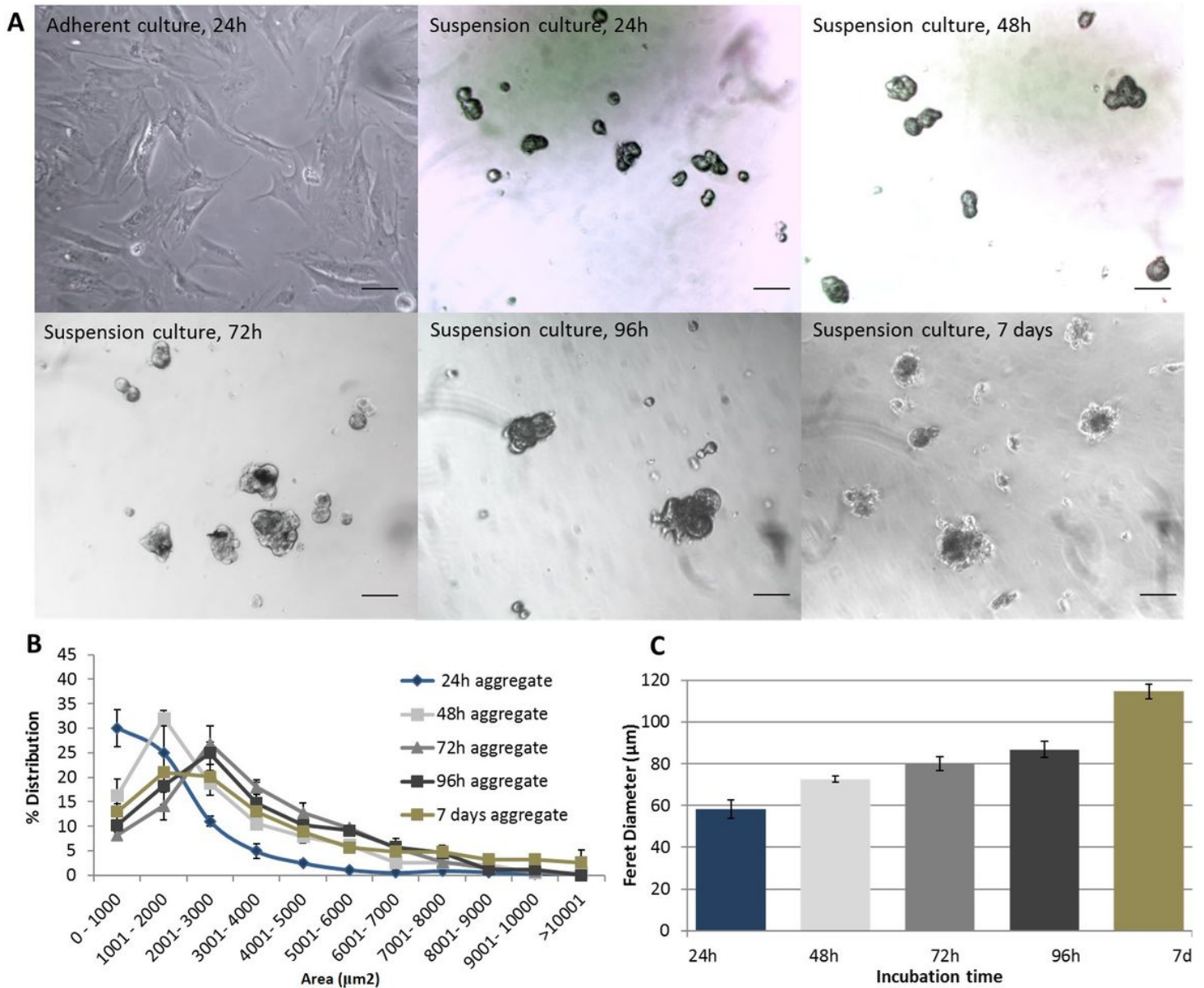


Figure 4

Time course of IPC/GPC aggregation formation. A) Optical microscopy of IPC/GPC. B) Area distribution of the cell aggregates. C) Feret diameter of cells aggregates. All experiments were performed at 24, 48, 72, 96 h and day 7 of culture. ANOVA followed by Student's t-test, $*p < 0.05$. n=4. Scale bar= 100 µm.

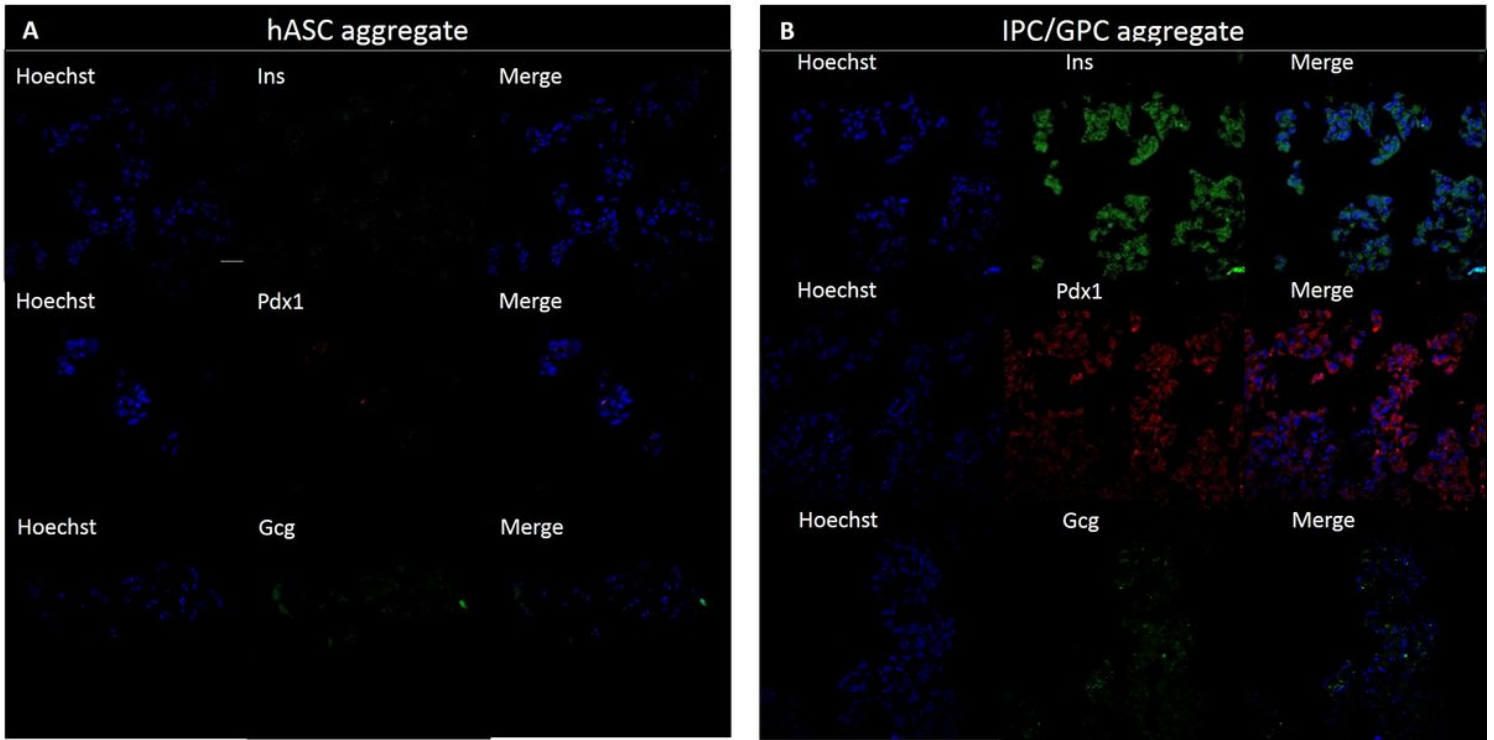


Figure 5

Expression of pancreatic markers in hASC and IPC/GPC aggregates at 72 h culture by indirect immunofluorescence. The images shown are representative of n=3 experiments, visualized by confocal microscopy. The left panel corresponds to cell aggregates of hASC and the right panel to cell aggregates of IPC/GPC. A) Insulin (green). B) Pdx1 (red) and C) Gcg (green). Hoechst staining 1:500 (blue) was performed to detect nuclei, n=3. Scale bar= 40 μ m.

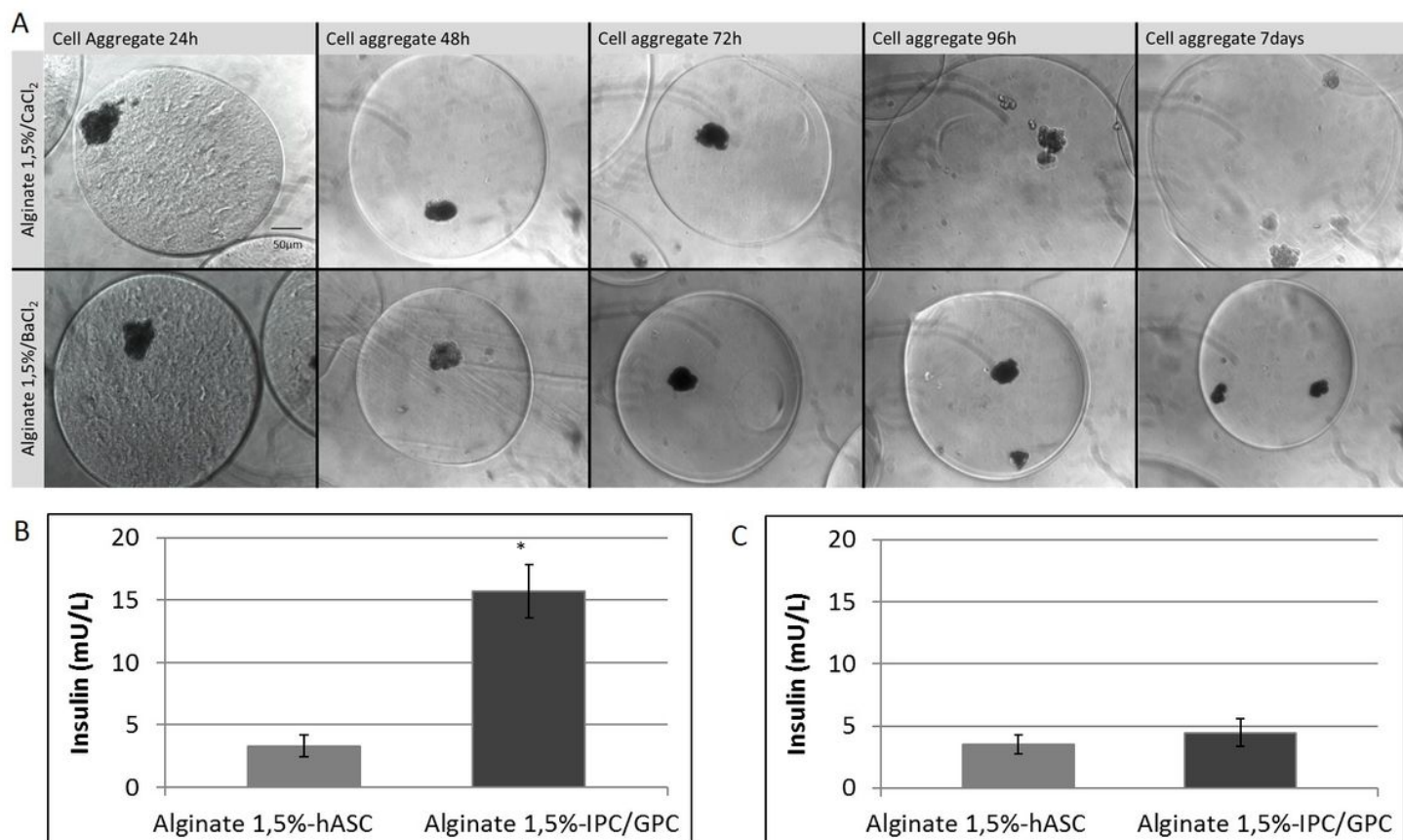


Figure 6

Characterization of IPC/GCP aggregates in microgels. Light microscopy was performed at different times for A) Calcium (upper panel) or Barium (lower panel). (n=5) B) Insulin secretion from microgels at 1 day (n=3) B) Insulin secretion from microgels at 7 days (n=3). Student's t-test, *p<0,05. Scale bar= 50 μ m.

Supplementary Files

This is a list of supplementary files associated with this preprint. Click to download.

- [FigS1.jpg](#)
- [FigS2.jpg](#)
- [SupplementalInformation2020withrevisionsfinal.pdf](#)
- [SupplementalInformation2020withrev4finalversion.docx](#)